Int. J. Solids Structures Vol. 23, No. 1, pp. 23–43, 1987
Printed in Great Britain.

0020-7683/87 $3.00 + .00
Pergamon Journals Ltd.

ELASTIC SOLIDS WITH MANY CRACKS: A SIMPLE METHOD OF ANALYSIS

MARK KACHANOV
Department of Mechanical Engineering, Tufts University, Medford, MA 02155, U.S.A.

(*Received* 16 *May* 1985; *in revised form* 20 *December* 1985)

Abstract—A simple method of stress analysis in elastic solids with many cracks is proposed. It is based on the superposition technique and the ideas of self-consistency applied to the average tractions on individual cracks. The method is applicable to both two- and three-dimensional crack arrays of arbitrary geometry. It yields approximate analytical solutions for the stress intensity factors (SIFs) accurate up to quite close distances between cracks. It is also suggested how a full stress field can be approximately constructed. Applications to a configuration "crack–microcrack array" and to a problem of effective elastic properties of a solid with cracks are considered.

1. INTRODUCTION

The problem of a linear elastic solid with N cracks having unit normals $\mathbf{n}_i$ and subjected to remote loading $\boldsymbol{\sigma}^\infty$ is equivalent to the problem with tractions $\mathbf{n}_i \cdot \boldsymbol{\sigma}^\infty$ applied to the crack faces and stresses vanishing at infinity. The latter problem, as well known, can be represented as a superposition of N problems, each involving only *one* crack but loaded by *unknown* tractions, induced, on a line of a given crack (in a continuous material), by other cracks and by remote loading.† These tractions can be interrelated through a system of integral equations. Approximate methods of solution of the mentioned system constitute, therefore, a possible approach to the crack interaction problems.

A simpler method of stress analysis in elastic solids with many cracks is proposed here (see also Ref. [1]). It is based on the superposition technique and the ideas of self-consistency applied to the average tractions on individual cracks. The method yields approximate analytical solutions applicable to both 2-D and 3-D crack arrays of arbitrary geometry. The accuracy generally depends on the density of cracks and remains good up to quite close distances between cracks (much smaller than the crack size).

The key simplifying assumption of our method is somewhat similar to the Saint-Venant principle of elasticity (see Discussion).

The presented method can be considered as a further development of the ideas of the earlier work[4–6] where tractions on individual cracks were interrelated by the self-consistency conditions. In this work, the system "crack–microcrack array" was analyzed; tractions on microcracks were approximated by Taylor's polynomials and the polynomial coefficients for different cracks were related through potential representations (applicable to both 2-D and 3-D configurations). Note that similar polynomial approximations for the general 2-D array of cracks and holes were used by Horii and Nemat-Nasser[7,8]; the same approach but with a different choice of approximating polynomials was also developed by Gross[3] and Chen[9]. Comparison of our method with the polynomial approximation techniques is given in Section 11.

The method is first illustrated on two "test" problems with known exact solutions and then formulated for a general crack array.

† Such representations were used by Datsyshin and Savruk[2] and, recently, by Gross[3], Chudrovsky and co-workers[4–6], Horii and Nemat-Nasser[7,8] (where they were called "the method of pseudotractions") and Chen[9]. In the displacements formulation, similar representations were used by Collins[10].

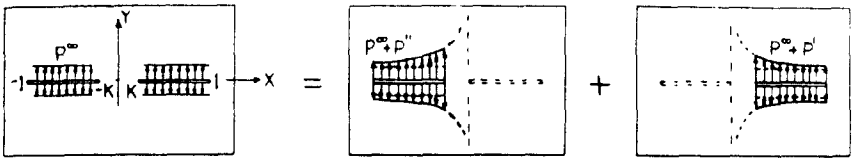

Fig. 1. Superposition for two collinear cracks.

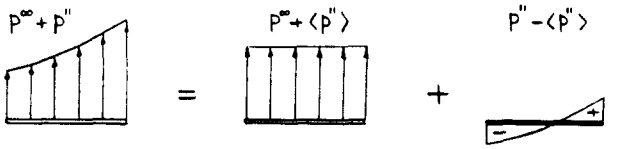

Fig. 2. Traction on a crack as a sum of its average and a nonuniformity having zero average.

2. TEST PROBLEM: TWO COLLINEAR CRACKS

The problem of two collinear cracks of equal length in an infinite plate loaded by uniform remote traction p^∞ has an exact analytical solution[11] and can, therefore, serve as a test for the proposed method.

The problem is equivalent to the following one: normal traction p^∞ is applied to the crack faces and stresses vanish at infinity. (Strictly speaking, the traction applied to the crack faces is $-p^\infty$, since it differs from the traction induced on the crack line in a continuous material by the minus sign. These minus signs are omitted below for convenience.) The latter problem can be represented as a superposition of two problems, each involving only one isolated crack but loaded by unknown tractions (see Fig. 1 where the parameter k characterizes the ratio of the distance $2k$ between cracks to the crack length $1 - k$). The traction on crack 2, $(k, 1)$ is

$$p_2(x) = p^\infty + p'(x) \tag{1}$$

where $p'(x)$ denotes the stress σ_{yy} generated along the line $(k, 1)$ in a continuous material by crack 1, the latter being loaded by

$$p_1(x) = p^\infty + p''(x) \tag{2}$$

where $p''(x)$ is the crack 2-generated stress. (Interrelating p' and p'' through integral equations would constitute a conventional approach to the problem.)

Represent $p_1(x)$ as a sum of its average $\langle p_1 \rangle = \langle p^\infty + p'' \rangle = p^\infty + \langle p'' \rangle$ and the difference $p'' - \langle p'' \rangle$ having zero average (Fig. 2). The key assumption of the method is to neglect the traction on crack 2 due to the load $p'' - \langle p'' \rangle$ on crack 1. Thus the stress shed on crack 2 by crack 1 results just from the uniform average traction on crack 1; the impact on crack 2 of the traction nonuniformities on crack 1 with a zero average is neglected. This assumption results in a major simplification of the problem. Indeed, the traction p' induced on crack 2 by crack 1 is then taken as the response of the latter to $\langle p_1 \rangle$ so that

$$p_2(x) = p^\infty + \langle p_1 \rangle \left[\frac{x + (1 + k)/2}{\sqrt{((x + k)(x + 1))}} - 1 \right] \tag{3}$$

where the expression in square brackets is the stress σ_{yy} generated by crack 1 loaded by a uniform normal traction of unit intensity (see, e.g. Ref. [12]). The stress intensity factors (SIFs) at the crack 2 tips would have been readily found if the average traction $\langle p_1 \rangle$ on crack 1 were known.

We introduce a *transmission factor* Λ defined as follows. Apply a uniform normal traction of unit intensity to the faces of crack 1 (considered as an isolated crack in an

Table 1. Comparison with the exact results for two collinear cracks

k	$K_I(k)/K_I^0$ (inner tip) Exact	As given by eqn (6)	Error (%)	$K_I(1)/K_I^0$ (outer tip) Exact	As given by eqn (6)	Error (%)
0.2	1.112	1.112		1.052	1.052	
0.1	1.255	1.251	0.3	1.086	1.086	
0.05	1.473	1.452	1.4	1.120	1.118	0.2
0.02	1.905	1.809	5.0	1.159	1.154	0.4
0.01	2.372	2.134	10	1.184	1.175	0.8

infinite plane). The traction $\sigma_{yy}(x)$ generated along the x-axis is given by the expression in square brackets in eqn (3). Its average taken along the line $(k, 1)$ in a continuous material is

$$\frac{1}{1-k}\int_k^1 \sigma_{yy}(x)\,dx = \frac{\sqrt{(2(1+k))}}{1+\sqrt{k}} - 1 \equiv \Lambda. \tag{4}$$

The factor Λ characterizes attenuation of the average traction in transmission of stress from crack 1 onto the crack 2 line. Note that $\Lambda < 1$ and decreases from $\sqrt{2}-1$ to 0 when k changes from 0 to 1. Obviously, Λ is the same in transmissions from crack 1 onto the crack 2 line and vice versa.

Now $\langle p_1 \rangle$ is readily found in terms of Λ: taking the average of eqn (1)

$$\langle p_2 \rangle = p^\infty + \langle p' \rangle = p^\infty + \Lambda \langle p_1 \rangle$$

together with the condition $\langle p_1 \rangle = \langle p_2 \rangle = \langle p \rangle$ (symmetry of the configuration) yields

$$\langle p \rangle = \frac{p^\infty}{1-\Lambda}. \tag{5}$$

Equation (5) shows an increase of the average traction due to crack interaction. Using the general formula, eqn (14), for the SIFs at the tips of a crack loaded by a given traction, the latter being taken from eqn (3), one obtains the following expressions for the SIFs at the outer and inner tips, correspondingly

$$K_I(1) = K_I^0\left\{1 + \frac{1}{1-\Lambda}\frac{1}{\pi(1-k)}\left[2\mathscr{E} - k(k+1)\mathscr{K} - \frac{\pi}{2}(1-k)\right]\right\}$$

$$K_I(k) = K_I^0\left\{1 + \frac{1}{1-\Lambda}\frac{1}{\pi(1-k)}\left[-2\mathscr{E} + (k+1)\mathscr{K} - \frac{\pi}{2}(1-k)\right]\right\} \tag{6}$$

where $K_I^0 = p^\infty\sqrt{(\pi(1-k)/2)}$ is the SIF for an isolated crack and $\mathscr{K}$, $\mathscr{E}$ are complete elliptic integrals of the argument $k' = \sqrt{(1-k^2)}$ of the first and second kind, respectively. This completes the solution.

These results are compared with the exact ones in Table 1. The agreement is very good. The error becomes noticeable for closely located cracks but even at $k = 0.05$ (distance between the cracks is one order of magnitude smaller than the crack length), the error is only 1.4% for $K_I(k)$ and 0.2% for $K_I(1)$.

A slight underestimation of K_I for closely located cracks is explained by the neglected response of crack 1 to the traction nonuniformity $p'' - \langle p'' \rangle$ on it. The tensile zone of this nonuniformity (marked by + in Fig. 2) would have generated some additional tensile traction along the crack 2 line.

Note that eqn (5) can be obtained in a somewhat different way. As a first step, we

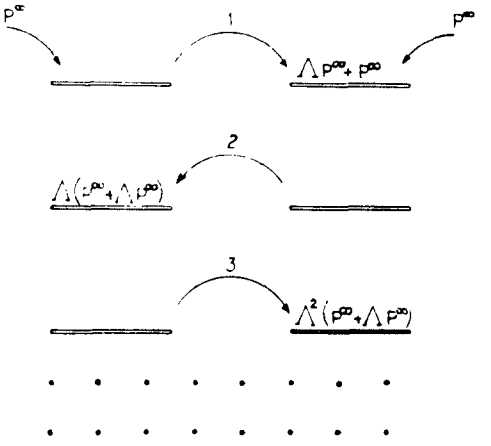

Fig. 3. "Feedback" loops for traction averages.

take the average traction on crack 2 as p^∞ plus the averaged response of crack 1 to p^∞, i.e. $p^\infty + \Lambda p^\infty$. Thus, we make an error in $\langle p_2 \rangle$ by not accounting for the "feedback" from crack 2. Taken as a response of crack 2 to the average traction $p^\infty + \Lambda p^\infty$, this feedback will generate the additional average traction $\Lambda(p^\infty + \Lambda p^\infty)$ on crack 1, which in turn will result in additional average traction $\Lambda^2(p^\infty + \Lambda p^\infty)$ on crack 2. The next feedback loops (Fig. 3 illustrates transmission of the averages) will bring the total average to a sum of the geometrical series

$$(p^\infty + \Lambda p^\infty) + \Lambda^2(p^\infty + \Lambda p^\infty) + \cdots = (p^\infty + \Lambda p^\infty)\frac{1}{1-\Lambda^2} = \frac{p^\infty}{1-\Lambda} \tag{7}$$

which coincides with eqn (5). Note that this procedure corresponds to solving the linear algebraic equation of self-consistency for the average traction $\langle p \rangle = p^\infty + \Lambda\langle p \rangle$ by iterations, with $\langle p \rangle = p^\infty$ being a zeroth iteration.

Generally, the iterations (and their interpretation in terms of "feedback loops") are unnecessary, since the system of linear algebraic equations for the traction averages on cracks (see Section 4) can be easily solved by direct means.

3. TEST PROBLEM: PERIODIC ROW OF CRACKS

As another test, we consider a periodic row of cracks in an infinite plate subjected to a remote tension p^∞. Representing the equivalent problem (with traction p^∞ applied to the crack faces and stresses vanishing at infinity) as a superposition of (identical) problems involving one crack each (Fig. 4), we write the traction on any given crack as a sum

$$p(x) = p^\infty + \sum_{k=-\infty,\, k\neq 0}^{\infty} p_k(x) \tag{8}$$

where $p_k(x)$ is the traction σ_{yy} generated by the kth crack; positive and negative indices k correspond to cracks on the left and on the right of the given crack, respectively.

In accordance with the key idea of the method, $p_k(x)$ is taken to be generated by the (yet unknown) uniform average traction $\langle p \rangle$ (the same for all cracks) acting on the kth crack. Then

$$p_k(x) = \langle p \rangle \left[\frac{|kh - x|}{\sqrt{((kh-x)^2 - l^2)}} - 1 \right] \tag{9}$$

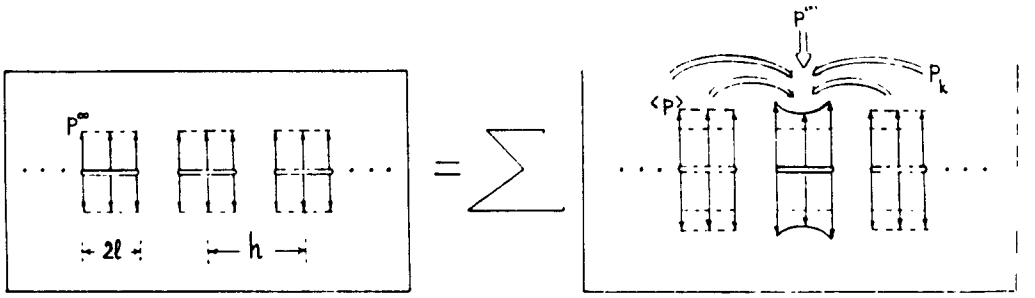

Fig. 4. Superposition for periodic row of cracks.

Table 2. Comparison with the exact results for a periodic row of collinear cracks

	K_1/K_1^0		
$\frac{h}{2l} - 1$	Exact	As given by eqn (9)	Error (%)
1.0	1.128	1.128	
0.5	1.286	1.286	
0.25	1.565	1.572	0.4
0.1	2.207	2.271	2.9
0.05	2.987	3.194	6.9
0.025	4.126	4.666	13
0.01	6.499	7.973	23

in the coordinate system with the origin at the center of the considered crack $(-l, l)$. Taking the average of eqn (9) over $(-l, l)$ yields the transmission factor $\Lambda^{(k)}$ characterizing the attenuation of the average traction in transmission of stresses from the kth crack onto the given crack

$$\Lambda^{(k)} = |k|\zeta(\sqrt{(1 + (1/|k|\zeta))} - \sqrt{(1 - (1/|k|\zeta))}) - 1$$

where $\zeta = h/2l$. Note that $\Lambda^{(k)} \sim (1/8\zeta^2)(1/k^2)$ for large k. Taking the average of eqn (8) over $(-l, l)$ results in the self-consistency equation for $\langle p \rangle$

$$\langle p \rangle = p^\infty + \sum_{\substack{k=-\infty \\ k \neq 0}}^{\infty} \Lambda^{(k)} \langle p \rangle = p^\infty + 2\langle p \rangle \sum_{k=1}^{\infty} \Lambda^{(k)}$$

from which we find

$$\langle p \rangle = \frac{p^\infty}{1 - 2\Sigma\Lambda^{(k)}} \tag{10}$$

thus expressing the average traction in terms of a sum of transmission factors.

The stress intensity factor K_1 is now readily found as generated by p^∞ and a sum of all the tractions (9), with $\langle p \rangle$ given by eqn (10). The ratio K_1/K_1^0 (where $K_1^0 = p^\infty\sqrt{(\pi l)}$) is compared with the exact analytical solution[11] in Table 2. The accuracy is quite good unless the distance between cracks becomes two orders of magnitude smaller than the crack length.

Note. Each of the considered test problems is a highly symmetric crack configuration. Therefore, the question arises: will our method work as well for the *arbitrary* crack array (see the next section)? Since the applicability of the method depends on the possibility to neglect the impact on a *given* crack of the traction nonuniformities (having zero average) on the *other* cracks, the accuracy depends on *distances* between cracks but not on the symmetry of configuration. In fact, the first test problem (two collinear cracks) presents a

difficult situation for the method. In this problem, the actual tractions deviate from their averages quite significantly: for $k = 0.05$, $p(x)$ varies from $1.94\,p^\infty$ to $1.07\,p^\infty$ along the crack 2 line, whereas the average value $\langle p\rangle = 1.23\,p^\infty$. In spite of such a variation, the accuracy is quite good. Note, also, that in the 3-D case, the method will yield accurate results at even closer distances, since the crack-generated stresses attenuate faster with distance.

4. ARBITRARY CRACK ARRAY

Application of the method to an arbitrary 2-D array of N cracks $l_1,\ldots,l_N$ with unit normals $\mathbf{n}_i$ and remote loading $\boldsymbol{\sigma}^\infty$ is straightforward. The equivalent problem—with the tractions $\mathbf{n}_i\cdot\boldsymbol{\sigma}^\infty$ applied to the ith crack faces and stresses vanishing at infinity—can be reduced, by superposition, to N problems, each containing one isolated crack loaded by unknown tractions. Problem 1, for instance, will contain the crack l_1 loaded by $\mathbf{n}_1\cdot\boldsymbol{\sigma}^\infty$ plus the sum of the tractions generated along the l_1-line by each of the cracks l_i (treated as isolated cracks in the otherwise continuous material).

According to the key idea of the method, we view traction induced along the l_1-line by crack l_i as resulting from (yet unknown) *uniform* average traction on l_i $(i = 2,\ldots,N)$. Modes I and II will be interrelated: normal (shear) loading of a crack will generate both normal and shear tractions along the other crack lines. Thus, denoting by p_i and τ_i the normal and shear tractions on l_i and by $\langle p_i\rangle$ and $\langle\tau_i\rangle$—their averages, we have the following tractions on crack l_1 ($-l_1 < \xi < l_1$ is a current point on l_1)

$$\begin{aligned} p_1(\xi) &= p_1^\infty + \mathbf{n}_1\cdot[\boldsymbol{\sigma}_2^n(\xi)\langle p_2\rangle + \boldsymbol{\sigma}_2^\tau(\xi)\langle\tau_2\rangle + \cdots + \boldsymbol{\sigma}_N^n(\xi)\langle p_N\rangle \\ &\quad + \boldsymbol{\sigma}_N^\tau(\xi)\langle\tau_N\rangle]\cdot\mathbf{n}_1 \\ \tau_1(\xi) &= \tau_1^\infty + \mathbf{n}_1\cdot[\boldsymbol{\sigma}_2^n(\xi)\langle p_2\rangle + \boldsymbol{\sigma}_2^\tau(\xi)\langle\tau_2\rangle + \cdots + \boldsymbol{\sigma}_N^n(\xi)\langle p_N\rangle \\ &\quad + \boldsymbol{\sigma}_N^\tau(\xi)\langle\tau_N\rangle]\cdot(\mathbf{I} - \mathbf{n}_1\mathbf{n}_1) \end{aligned} \tag{11}$$

where $p_1^\infty = \mathbf{n}_1\cdot\boldsymbol{\sigma}^\infty\cdot\mathbf{n}_1$ and $\tau_1^\infty = \mathbf{n}_1\cdot\boldsymbol{\sigma}^\infty\cdot(\mathbf{I} - \mathbf{n}_1\mathbf{n}_1)$ are the normal and shear tractions induced on l_1 by the remote loading ($\mathbf{I}$ and $\mathbf{n}_1\mathbf{n}_1$ denote a unit tensor and dyadic product of two vectors $\mathbf{n}_1$); $\boldsymbol{\sigma}_i^n$, $\boldsymbol{\sigma}_i^\tau$ are the stress fields generated by the ith crack loaded by uniform tractions (normal and shear, correspondingly) of unit intensity; they are "standard" fields given by elementary functions (see, e.g. Ref. [12] or appendix). The quantity in square brackets is the stress tensor induced along l_1 by the other cracks loaded by the traction averages on them.

Averaging eqns (11) along l_1 yields†

$$\begin{aligned} \langle p_1\rangle &= p_1^\infty + \Lambda_{21}^{nn}\langle p_2\rangle + \Lambda_{21}^{n\tau}\langle\tau_2\rangle + \cdots + \Lambda_{N1}^{nn}\langle p_N\rangle + \Lambda_{N1}^{n\tau}\langle\tau_N\rangle \\ \langle\tau_1\rangle &= \tau_1^\infty + \Lambda_{21}^{\tau n}\langle p_2\rangle + \Lambda_{21}^{\tau\tau}\langle\tau_2\rangle + \cdots + \Lambda_{N1}^{\tau n}\langle p_N\rangle + \Lambda_{N1}^{\tau\tau}\langle\tau_N\rangle \end{aligned} \tag{12}$$

where the transmission Λ-factors characterize transmission of the average normal and shear tractions; e.g. $\Lambda_{13}^{n\tau}$ is the average *shear* traction on crack l_3 resulting from the *normal* uniform load of unit intensity on crack l_1.

Equations (12) and similar equations on $l_2,\ldots,l_N$ constitute a system of $2N$ linear algebraic equations ("self-consistency" equations) for the average tractions $\langle p_k\rangle$, $\langle\tau_k\rangle$. Denoting by $\langle\mathbf{t}_k\rangle = (\langle p_k\rangle, \langle\tau_k\rangle)$ the average traction *vector* on the kth crack, we can write this system in a form of N vectorial linear algebraic equations

† Shear tractions τ_i are treated in eqn (12) as scalars; τ_i is taken as positive if its direction is consistent with the direction of shear traction generating a "standard" field $\boldsymbol{\sigma}_i^\tau$.

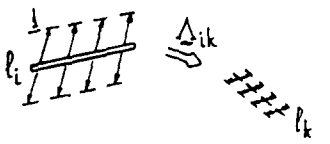

Fig. 5. Tensorial transmission factor.

$$\langle \mathbf{t}_k \rangle = \mathbf{t}_k^{\infty} + \boldsymbol{\Lambda}_{ik} \cdot \langle \mathbf{t}_i \rangle \qquad (\text{sum over } i = 1, \ldots, N; i \neq k) \tag{13a}$$

where the tensorial element $\boldsymbol{\Lambda}_{ik}$ gives the average traction vector generated along the kth crack line by an (isolated) ith crack loaded by a uniform traction of arbitrary direction and unit intensity (Fig. 5). It is given by the expression

$$\boldsymbol{\Lambda}_{ik} = \mathbf{n}_k \cdot \langle \boldsymbol{\sigma}_i^n \mathbf{n}_i + \boldsymbol{\sigma}_i^{\tau} \boldsymbol{\gamma}_i \rangle_{l_k} \qquad (\text{no sum over } i \text{ or } k)$$

involving averaging of the "standard" stress fields $\boldsymbol{\sigma}_i^n$, $\boldsymbol{\sigma}_i^{\tau}$ generated by the ith crack over l_k ($\boldsymbol{\gamma}_i$ is a unit vector tangent to l_i and $\boldsymbol{\sigma}_i^n \mathbf{n}_i$, $\boldsymbol{\sigma}_i^{\tau} \boldsymbol{\gamma}_i$ are dyadic (tensor) products). Noting that the diagonal elements $\boldsymbol{\Lambda}_{11}$, $\boldsymbol{\Lambda}_{22}$, ... characterizing the "interaction of a crack with itself" are unit tensors $\mathbf{I}$, we can rewrite eqn (13a) in a compact form

$$(\delta_{ik}\mathbf{I} - \boldsymbol{\Lambda}_{ik}) \cdot \langle \mathbf{t}_i \rangle = \mathbf{t}_k^{\infty} \tag{13b}$$

where the conventional summation agreement over all $i = 1, \ldots, N$ is observed.

Thus, crack interactions are described, in the framework of our method, by the *interaction matrix* $[\boldsymbol{\Lambda}_{ik}]$. It is, generally, nonsymmetric: $\boldsymbol{\Lambda}_{ik} \neq \boldsymbol{\Lambda}_{ki}$ (for instance, the impact of a large crack on a small one is larger than vice versa).

Note that the interaction matrix $[\boldsymbol{\Lambda}_{ik}]$ provides an *intrinsic description* of the crack array, reflecting its geometry but independent of the remote loading conditions; the latter affect only the right-hand parts of eqn (13b).

After the average tractions $\langle \mathbf{t}_i \rangle$ are determined from this system, tractions $p_i(\xi)$, $\tau_i(\xi)$ on cracks are found from eqn (11) and similar equations for $l_2, \ldots, l_N$; the SIFs are readily obtained from

$$\left.\begin{matrix} K_{\mathrm{I}}(\pm l_1) \\ K_{\mathrm{II}}(\pm l_1) \end{matrix}\right\} = \frac{1}{\sqrt{(\pi l_1)}} \int_{-l_1}^{l_1} \sqrt{\left(\frac{l_1 \pm \xi}{l_1 \mp \xi}\right)} \left\{\begin{matrix} p_1(\xi) \\ \tau_1(\xi) \end{matrix}\right\} \mathrm{d}\xi. \tag{14}$$

Depending on geometry of the crack array and loading conditions, crack interactions may result in both stress "shielding" (decrease of SIFs) and stress "amplification" (increase of SIFs). The test problems of Sections 2 and 3 represent the amplifying configurations whereas Section 7 contains 3-D examples of both shielding and amplification. The effects of shielding and amplification in the application to the "crack–microcrack array" configuration are considered in detail in Refs [18, 19].

Mode III loading can be analyzed along the same lines. Since it does not interact with modes I and II, the mode III analysis can be done separately.

In the 3-D case, the method remains essentially unchanged; the "standard" stress fields may be given by special, rather than elementary, functions and the SIFs (generally variable along the crack edges) are to be found by the 3-D analogues of integrations (14). The method can, therefore, be applied to arbitrary arrays of elliptical cracks (for which the "standard" field generated by a uniform loading on a crack is known).

Thus, the method involves: (a) finding the transmission factors, by averaging the "standard" stress fields generated by uniformly loaded cracks along the lines of other cracks, (b) solving a system of linear algebraic equations of self-consistency for the average tractions, and (c) finding the SIFs by integrations similar to (14).

5. WEAK CRACK INTERACTIONS

The test problems considered above show that the errors in SIFs vanish as the distance between cracks increases and interactions become weak. This fact is general: the method is *asymptotically exact* for weak crack interactions. We call the interactions *weak* if the average tractions $\langle \Delta p \rangle$, $\langle \Delta \tau \rangle$ induced on each crack by the other cracks are small as compared to the σ^{∞}-induced p^{∞}, τ^{∞}. Then all the transmission factors $\Lambda \ll 1$ and, to within small values of higher order, the traction on a given crack is a sum of $\mathbf{n} \cdot \boldsymbol{\sigma}^{\infty}$ and the tractions induced on it by the other cracks, *the latter being embedded in the* $\boldsymbol{\sigma}^{\infty}$*-field.* (This follows as a first-order solution of system (11) obtained by one iteration, with $p_i(\xi) = p_i^{\infty}$, $\tau_i(\xi) = \tau_i^{\infty}$ being an obvious zeroth iteration.) Thus, instead of

$$\mathbf{t}_k(\xi) = \mathbf{t}_k^{\infty} + \mathbf{n}_k \cdot \sum_i (\langle p_i \rangle \boldsymbol{\sigma}_i^n + \langle \tau_i \rangle \boldsymbol{\sigma}_i^{\tau}) \tag{15a}$$

(vectorial form of (11)), we have

$$\mathbf{t}_k(\xi) = \mathbf{t}_k^{\infty} + \mathbf{n}_k \cdot \sum_i (p_i^{\infty} \boldsymbol{\sigma}_i^n + \tau_i^{\infty} \boldsymbol{\sigma}_i^{\tau}) \tag{15b}$$

so that finding traction averages becomes unnecessary.

Applicability of the approximation of weak interactions depends on whether the inequalities for tractions $(\langle \Delta p \rangle, \langle \Delta \tau \rangle) \ll (p^{\infty}, \tau^{\infty})$ hold; they are much less restrictive than the geometrical condition (distances between cracks) $\gg$ (crack sizes) and, depending on the geometry of the crack array, may be satisfied for relatively closely located cracks.

As an illustration, consider again the test problem of two collinear cracks. Although the approximation of weak interactions yields error in SIFs substantially larger than the basic version of the method, this error is still less than 3% at $k = 0.1$ when the distance between cracks is 2/9 of the crack length.

In the 3-D case, the crack-generated stresses attenuate faster and the approximation of weak interactions can be applied to even closer distances between cracks.

6. REMOTELY LOCATED CRACKS

As noted above, the condition of weak interactions $(\langle \Delta p \rangle, \langle \Delta \tau \rangle) \ll (p^{\infty}, \tau^{\infty})$ does not impose any explicit conditions on the geometry of the crack array and is much less restrictive than the assumption of remotely located cracks (distances between cracks $\gg$ crack sizes). If, however, the latter assumption is made, further simplifications result and the solutions become quite elementary.

Since gradients of the stresses generated by cracks attenuate faster than the stresses themselves, the traction induced on a given crack line by the other cracks can be taken approximately constant. This constant can be taken, to within small values of a higher order, as the traction $\mathbf{n}_i \cdot \sum_{k \neq i} \boldsymbol{\sigma}_k(O_i)$ evaluated at the center O_i of the given crack l_i, where the "standard" fields $\boldsymbol{\sigma}_k$ can be substituted by their remote asymptotics.

Therefore, both averaging of the "standard" fields and solving a system of linear algebraic equations for averages become unnecessary and the procedure is reduced to evaluation of the remote "standard" fields at the centers of other cracks.

In this approximation, the SIFs at both crack tips of a given crack (2-D configurations) are the same. In the 3-D cases, mode I SIFs are constant along the crack edges whereas mode II and III SIFs undergo a variation along the edge corresponding to a constant shear traction. Examples are given in Section 7.

The approximation of remotely located cracks, as defined above, should be distinguished from the so-called "small concentration" approximation (terminology often used in models for the effective elastic properties of a medium with cracks). The latter treats

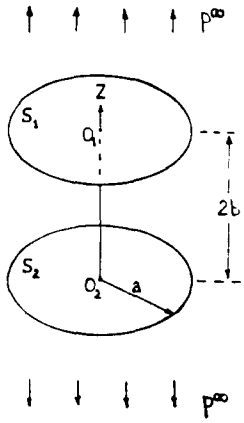

Fig. 6. Two parallel penny-shaped cracks.

each crack as embedded into the remotely applied field σ^∞; stress fields generated by the cracks are simply summed up, and crack interactions are entirely neglected. The approximation of remotely located cracks, on the other hand, provides a first-order correction due to crack interactions.

Note that this first-order correction depends not only on the density of cracks and their orientations but on their *mutual locations* (statistics of the crack centers) as well. The latter can be disregarded in the approximation of noninteracting cracks (infinitesimal crack density) only. This remark may be relevant for the problem of effective elastic properties of cracked solids at finite crack densities.

7. EXAMPLES IN 3-D (PENNY-SHAPED CRACKS)

7.1. *Remotely located cracks*

7.1.1. *Two parallel cracks of equal size* (*Fig.* 6). An explicit closed form solution of this problem has not been derived, to the best of our knowledge, but asymptotic estimates for the case $a/b \ll 1$ have been obtained by lengthy calculations[10]. In this case, the estimate of K_I can be obtained by very simple means in the framework of our method in the remote locations approximation. The traction p'' induced on S_1 by crack S_2 can be taken, to within small values of higher order, as the σ_{zz}-response of crack 2 to the uniform loading p^∞ evaluated at O_1, i.e. the stress generated along the Z-axis (see Ref. [12] or appendix)

$$\sigma_{zz} = \frac{2}{\pi} p^\infty \int_0^1 \frac{\rho\sqrt{(1-\rho^2)}}{(\rho^2+\bar{z}^2)^{3/2}}\left[1 + 6\frac{\bar{z}^2}{\rho^2+\bar{z}^2} - 15\frac{\bar{z}^4}{(\rho^2+\bar{z}^2)^2}\right]d\rho \tag{16}$$

($\rho = r/a$, $\bar{z} = z/a$) evaluated at $\bar{z} = 2b/a$. For $\bar{z} \gg 1$ we obtain

$$p'' = \sigma_{zz}(O_1) \approx -\frac{2}{\pi} p^\infty \int_0^1 \rho\sqrt{(1-\rho^2)}\left(\frac{a}{b}\right)^3 d\rho = -\frac{2}{3\pi}\left(\frac{a}{b}\right)^3 p^\infty \tag{17}$$

so that, to within small values of higher order in a/b

$$K_I = K_I^0\left[1 - \frac{2}{3\pi}\left(\frac{a}{b}\right)^3\right]. \tag{18}$$

This result coincides with the asymptotic estimate given in Ref. [13]. Note that the only information needed to obtain eqn (18) is the stress (17), generated by an isolated uniformly loaded crack at remote points above its center.

The restriction $a/b \ll 1$ can be removed and strong interaction can be considered by

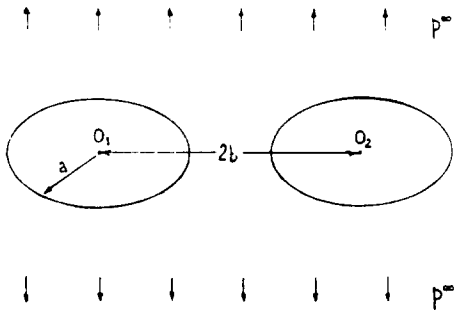

Fig. 7. Two co-planar penny-shaped cracks.

taking $p'' = p''(x, y)$ as the stress field generated on S_1 by crack S_2 loaded by $\langle p \rangle$, the latter being determined from the condition of self-consistency for the averages.

7.1.2. *Two parallel cracks of different radii, a_1 and a_2.* Taking traction induced on S_1 by crack S_2 as the crack S_2 response to the p^∞-loading evaluated at O_1, and following the same reasoning as above, we obtain $K_I^{(1)}$ on crack S_1

$$K_I^{(1)} = K_I^{(1)0}\left[1 - \frac{2}{3\pi}\left(\frac{a_2}{b}\right)^3\right]$$

and similarly for crack S_2

$$K_I^{(2)} = K_I^{(2)0}\left[1 - \frac{2}{3\pi}\left(\frac{a_1}{b}\right)^3\right].$$

7.1.3. *Two co-planar cracks* (*Fig.* 7). In the same approximation of remotely located cracks, evaluating the traction $p''(O_1)$ generated by crack 2 loaded by p^∞ at point O_1 from the expression for σ_{zz} in the plane of the crack (appendix)

$$\sigma_{zz} = \frac{2}{\pi} p^\infty \frac{1}{\sqrt{(\rho^2 - 1)}}[1 - \sqrt{(\rho^2 - 1)}\arctan(\rho^2 - 1)^{-1/2}] \tag{19}$$

($\rho = r/a$) for the remote points $2b/a \gg 1$, we obtain: $p''(O_1) = p^\infty(a/b)^3/12\pi$ so that, to within small values of higher order in a/b, K_I is constant along the crack edge and is given by

$$K_I = K_I^0[1 + (a/b)^3/12\pi]. \tag{20}$$

The second term in square brackets represents the stress "amplification" due to crack interaction. Comparison with the 2-D case (two collinear cracks) for which the similar asymptotic estimate yields

$$K_I = K_I^0[1 + (a/b)^2/8]$$

shows that the interaction is substantially weaker in the 3-D case, at least for remotely located cracks.

It is interesting to compare the stress amplification given by eqn (20) with the stress "shielding" (decrease in K_I due to interaction of cracks) for the stacked cracks, eqn (18). The effect of shielding is much more pronounced (8 times) for the same ratios a/b.

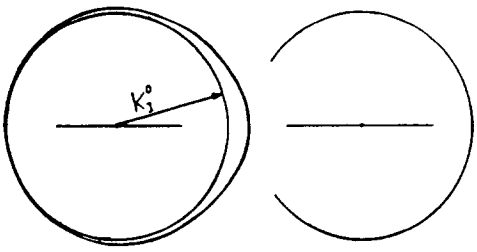

Fig. 8. Strong interaction of two co-planar cracks (distance between cracks equals 1/10 of the crack diameter). Variation of K_I/K_I^0 around the crack edge.

7.1.4. *Two co-planar cracks of different radii, a_1 and a_2.* The same considerations as for the stacked cracks yield

$$K_I^{(1)} = K_I^{(1)0}[1 + (a_2/b)^3/12\pi], \qquad K_I^{(2)} = K_I^{(2)0}[1 + (a_1/b)^3/12\pi].$$

7.2. *Closely located co-planar cracks (strong interaction)*

In the case of strong interaction (closely located cracks), we use the full expression, eqn (19), rather than its remote asymptotics; the average traction $\langle p \rangle$ (the same for both cracks) is found from the self-consistency condition and then eqn (19) (with $\langle p \rangle$ in the place of p^∞) is integrated (3-D analogue of (14)) along the surface of the crack. The result (K_I varying along the crack edge) is shown in Fig. 8 for the case when the distance between cracks equals 1/10 of the crack diameter. At such distances, the errors $\approx 1\%$ in the corresponding 2-D problem (Table 1); in 3-D, the errors are generally smaller (crack-generated stresses attenuate faster with distance). The results of Fig. 8 are therefore expected to be quite accurate.

The maximal increase in K_I along the crack edge, due to interaction, is about 17%. Note that in the corresponding 2-D problem (Fig. 1) with the same ratio of the distance between cracks to the crack size, the increase in K_I at the inner tips is about 50%. This illustrates the fact that crack interactions are generally weaker in 3-D configurations as compared to 2-D ones.

8. CONSTRUCTION OF A FULL STRESS FIELD

The presented method yields the SIFs and average tractions on cracks. In the 2-D case, these quantities can be used to construct the full stress field in a solid, by the procedure outlined below. Since stresses corresponding to the given SIFs and traction averages can be determined only to within a stress field generated by any system of loads resulting in zero SIFs and traction averages, such a construction is, obviously, only an approximation of the actual field.

The displacement field generated by a single crack can be represented as an integral of the double layer potential type (also known as a representation of a crack by dislocations)

$$\mathbf{u}(\mathbf{x}) = \int_{-l}^{l} \mathbf{b}(\xi) \cdot \mathbf{\Phi}(\xi, \mathbf{x})\, d\xi \tag{21}$$

where $\mathbf{b}(\xi)$ is the displacement discontinuity (crack opening displacement, COD); it is vectorial since both modes I and II may be present; and $\mathbf{\Phi}$ is the second Green's tensor of elasticity for an infinite plane. Differentiation of $\mathbf{u}(\mathbf{x})$ (can be applied to $\mathbf{\Phi}$ under the integral) and multiplication by the appropriate elastic constants yield the stress field $\boldsymbol{\sigma}(\mathbf{x})$ if $\mathbf{b}(\xi)$ is known. In the case of N cracks, the $\mathbf{u}$- and $\boldsymbol{\sigma}$-fields are given by a sum of integrals (21) taken over all l_i so that the problem would have been solved if the CODs were known.

We suggest constructing each of the normal b_n (tangential b_τ) components of the COD of a given crack $-l < x < l$ as an ellipse that would correspond to a certain uniform

normal (shear) loading multiplied by a quadratic polynomial ("polynomially distorted" ellipse)

$$b_n = \frac{4l}{E'}\sigma_n\left(1 + \alpha_n\frac{x}{l} + \beta_n\frac{x^2}{l^2}\right)\sqrt{\left(1 - \frac{x^2}{l^2}\right)}$$

$$b_\tau = \frac{4l}{E'}\sigma_\tau\left(1 + \alpha_\tau\frac{x}{l} + \beta_\tau\frac{x^2}{l^2}\right)\sqrt{\left(1 - \frac{x^2}{l^2}\right)} \tag{22}$$

(E' is Young's modulus E for plane stress and $E/(1-\nu)$ for plane strain) where the three coefficients of the quadratic polynomials in each of the modes (σ_n, α_n, β_n and σ_τ, α_τ, β_τ) are chosen in such a way as to match the previously found values of the SIFs and average tractions ($K_I(\pm l)$, $\langle p\rangle$ and $K_{II}(\pm l)$, $\langle\tau\rangle$), i.e. (appendix)

$$\left.\begin{aligned}
\sigma_n &= \langle 2p\rangle - \frac{K_I(l) + K_I(-l)}{2\sqrt{(\pi l)}} \\
\alpha_n &= \frac{K_I(l) - K_I(-l)}{4\langle p\rangle\sqrt{(\pi l)} - [K_I(l) + K_I(-l)]} \\
\beta_n &= 2\frac{K_I(l) + K_I(-l) - 2\langle p\rangle\sqrt{(\pi l)}}{4\langle p\rangle\sqrt{(\pi l)} - [K_I(l) + K_I(-l)]}.
\end{aligned}\right\} \tag{23}$$

(Identical formulas hold for the mode II quantities.)

Substitution of thus found $\mathbf{b}(x)$ into the integral representation (21) results in a stress field expressed in elementary functions (appendix).

Note that the idea of a "polynomially distorted" ellipse can be related to the polynomial conservation theorem stating that a crack loaded by a traction polynomial of degree N assumes the shape of an ellipse times a certain "distortion" polynomial of the same degree N. The shape (22) corresponds, therefore, to an approximation of the tractions induced on a given crack line by other cracks by a certain quadratic polynomial, namely (appendix)

$$p(x) = \sigma_n\left(1 - \frac{\beta_n}{2} + 2\alpha_n\frac{x}{l} + 3\beta_n\frac{x^2}{l^2}\right), \qquad \tau(x) = \sigma_\tau\left(1 - \frac{\beta_\tau}{2} + 2\alpha_\tau\frac{x}{l} + 3\beta_\tau\frac{x^2}{l^2}\right) \tag{24}$$

with α, β given by eqns (23); these tractions "match" the previously found values of the stress intensity factors and average traction on the given crack. If the polynomial approximation (24) were based on the *exact* values of SIFs and the traction averages then the difference between the constructed and the actual stress fields would have amounted to a stress field generated by such a system of tractions on the cracks that (a) all the SIFs were equal to zero, and (b) traction averages on each of the crack faces were equal to zero. Such a stress field can be expected to be just a small perturbation of the actual field except, possibly, in the close vicinity of the crack faces (where the boundary conditions are not exactly satisfied). If the values of SIFs and traction averages used in eqns (23) are sufficiently close to the actual ones, then the relative error in the stress field can still be expected to be small.

As an example, consider again the problem of two collinear cracks (Fig. 1), for which the exact shape of the COD is given in Ref. [12] for $k = 0.1$ (Fig. 9, solid line); note that, in the scale used, this shape deviates substantially from the elliptical COD for one isolated crack. Figure 9 (dashed line) shows the "quadratically distorted" ellipse, with the distortion polynomial found from eqns (22) and (23). Except in the vicinity of the point $x = 0.7$ where a slight deviation occurs, the constructed shape coincides with the actual COD to within the thickness of the line. This test problem seems to indicate that the "quadratically distorted" ellipse, chosen as to match the SIFs and average tractions, is a reasonable

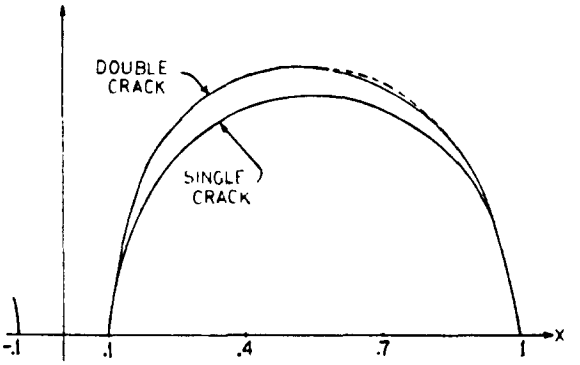

Fig. 9. COD in the problem of two collinear cracks (solid line, actual shape of the cracks; dashed line, "quadratically distorted" ellipse).

approximation of the actual COD. Applying it to the CODs in a solid with many cracks and using potential representations—sums of integrals (21), one may obtain a reasonable approximation of the fields $\mathbf{u}(\mathbf{x})$ and $\sigma(\mathbf{x})$.

9. ON THE PROBLEM OF EFFECTIVE ELASTIC PROPERTIES OF SOLIDS WITH CRACKS

Below, we outline how to apply the presented method to the problem of effective elastic properties of solids with cracks.

The problem is formulated as finding a fourth rank tensor $\mathbf{C}^{\text{eff}}$ relating the average over a representative volume V strain $\langle\varepsilon\rangle$ to the remotely applied stress σ^{∞} (which is also equal to the volume average $\langle\sigma\rangle$ [14])

$$\langle\varepsilon\rangle = \mathbf{C}^{\text{eff}}:\sigma^{\infty}. \tag{25}$$

(The semicolon denotes contraction over two indices.) The commonly used starting point is a representation of $\langle\varepsilon\rangle$ in the form

$$\langle\varepsilon\rangle = \mathbf{C}^{0}:\sigma^{\infty} + \frac{1}{2V}\sum_i \int_{S_i} (\mathbf{nb} + \mathbf{bn})\,dS.$$

Notations are as follows: $\mathbf{C}^0$ is a tensor of elastic compliance of the material without cracks; $\mathbf{n}_i$ is a unit normal to the ith crack with a surface S_i; $\mathbf{b}_i$ is the displacement discontinuity across S_i (relative displacement of the crack faces), it is vectorial since both normal and tangential components may be present.

For *flat* cracks, $\mathbf{n}$ = const along each of the cracks so that

$$\langle\varepsilon\rangle = \mathbf{C}^{0}:\sigma^{\infty} + \frac{1}{2V}\sum_i (\mathbf{n}\langle\mathbf{b}\rangle + \langle\mathbf{b}\rangle\mathbf{n})_i S_i \tag{26}$$

where $\langle\mathbf{b}_i\rangle$ denotes the average of $\mathbf{b}_i$ over S_i. In the 2-D case, surfaces S_i are to be substituted by lines l_i and representative volume V by representative area A.

Thus, the problem is reduced to the determination of the average displacement discontinuities $\langle\mathbf{b}_i\rangle$ on cracks; if we could relate them to σ^{∞} and to the crack array geometry, the effective elastic properties $\mathbf{C}^{\text{eff}}$ would have been found.

The existing models, aside from the approximation of noninteracting cracks (small crack density) belong to one of the modifications of the self-consistent or differential schemes. Limitations and certain conceptual difficulties of these models were discussed in a recent survey by Hashin[15]. Note, also, that it appears difficult to incorporate the information on *mutual locations* of cracks (statistics of crack centers) into these schemes.

A new approach to the problem, based on the presented method can be suggested. The problem that arises is to relate the average displacement discontinuities $\langle \mathbf{b}_i \rangle$ in eqn (26) to the quantities $K(\pm l_i)$ and $\langle \mathbf{t}_i \rangle$ (SIFs and average tractions on cracks) provided by the method.

Such a relationship can be established, in the 2-D case, by taking averages of the CODs given by eqns (22) and making use of eqns (23); this would express $\langle \mathbf{b}_i \rangle$ in terms of $K(\pm l_i)$ and $\langle \mathbf{t}_i \rangle$. The example of two collinear cracks appears to be encouraging: Fig. 9 (and the identical figure for the mode II COD) shows that the areas under the dashed and solid lines differ negligibly; note that cracks represented in Fig. 9 are located quite closely: (distance between cracks)/(crack length) = 2/9. The averages (integrals) of eqns (22) are expressed in elementary functions, and the effective properties are found by relatively elementary means. For the 3-D crack arrays, where the SIFs are variable along the crack edges, establishing relationships similar to eqns (22)–(24) is, presently, less clear.

An even simpler, and physically interesting, way to establish a relation for $\langle \mathbf{b} \rangle$ (applicable to both 2-D and 3-D configurations) can be suggested as follows. In the 2-D case, direct calculations of $\langle b_n \rangle$ from eqns (22) yields

$$\langle b_n \rangle = \pi \frac{l}{E'} \sigma \left(1 + \frac{\beta}{4} \right). \tag{27}$$

On the other hand, calculations show that if $p(x)$ is the traction that would have produced $b_n(x)$ given by eqns (22), then its average is

$$\langle p \rangle = \sigma_n \left(1 + \frac{\beta}{3} \right). \tag{28}$$

Thus

$$\langle b_n \rangle = \langle p \rangle \cdot \frac{\pi l}{E'} \cdot \frac{1 + \beta/4}{1 + \beta/3}. \tag{29}$$

The ratio $(1 + \beta/4)/(1 + \beta/3)$ depends on the coefficient β at the quadratic term in the distortion polynomial (note that it does not depend on the coefficient at the linear term) but, typically, it does not deviate much from 1. In the example of Fig. 9, $\beta = 0.22$ so that the mentioned ratio differs from 1 by less than 2%. Note that at even much larger β, of the order of 1, that may occur at very close distances between cracks, this ratio is still ≈ 1 to within a few percent. This, together with the fact that the mode II quantities, $\langle b_\tau \rangle$ and $\langle \tau \rangle$, are interrelated by the formula analogous to eqn (29), lead to a simple proportionality relation for the vectorial quantities†

$$\langle \mathbf{b} \rangle \approx \frac{\pi l}{E'} \langle \mathbf{t} \rangle. \tag{30}$$

Finding $\langle \mathbf{t} \rangle$'s from eqn (13b) and substituting into eqns (30) and (26) yield the following expression for $\mathbf{C}^{\text{eff}}$:

$$C^{pqrs} = C^{(0)pqrs} + \frac{l_i l_i}{2A} (\Omega_{ik}^{qr} n_i^p n_k^s + \Omega_{ik}^{ps} n_i^q n_k^r) \tag{31}$$

where $\mathbf{\Omega}_{ik} = (\delta_{ik}\mathbf{I} - \mathbf{\Lambda}_{ik})^{-1}$ and summation over the crack numbers i, k is assumed.

† Note that formulas (29) and (30) will not change if the quadratic approximation, eqns (24), of tractions on a given crack (and, correspondingly, "quadratically distorted" COD ellipses, eqns (22)) is upgraded to a *cubic* one, since the odd order polynomial terms do not affect the average quantities $\langle \mathbf{b}_i \rangle$ and $\langle \mathbf{t}_i \rangle$.

In the 3-D case (penny-shaped cracks) the normal and shear "compliances" of a crack (i.e. the average normal and shear relative displacements of the crack faces resulting from the unit normal and shear tractions) are not the same so that the vectors $\langle \mathbf{b} \rangle$ and $\langle \mathbf{t} \rangle$ are not collinear (although the angle between them is relatively small). Therefore, a relation of the type of eqn (30) ought to be formulated for the normal and shear components separately and for a crack of radius R we have

$$\langle \mathbf{b} \rangle = \langle \mathbf{b}_n \rangle + \langle \mathbf{b}_\tau \rangle = \beta \langle \mathbf{t} \rangle \cdot \mathbf{nn} + \gamma \langle \mathbf{t} \rangle \cdot (\mathbf{I} - \mathbf{nn}) \tag{32}$$

where $\beta = 16(1 - \nu^2)R/3\pi E$ and $\gamma = 32(1 - \nu^2)R/3\pi(2 - \nu)E$ are the normal and shear "compliances" of the crack. Finding the average traction $\langle \mathbf{t}_i \rangle$ on the ith crack from eqn (13b) and substituting into eqns (32) and (26) yield:

$$C^{pqrs} = C^{(0)pqrs} + \frac{16(1 - \nu^2)}{3\pi(2 - \nu)E} \frac{S_i R_i}{V} (\Omega_{ik}^{ps} n_i^q n_k^r + \Omega_{ik}^{qr} n_i^p n_k^s - \nu \Omega_{ik}^{ir} n_i^l n_i^p n_i^q n_k^s) \tag{33}$$

where the summation over the crack numbers i, k is assumed and $S_i = \pi R_i^2$ is the crack area.

Formulas (31) and (33) are explicit expressions for the effective elastic properties. They are given in terms of Ω's, i.e. the problem is reduced simply to inversion of the matrix of transmission factors.

The simplest approximation of non-interacting cracks (called sometimes a small crack density approximation) when each crack is assumed to be embedded into the σ^∞-field ($\langle \mathbf{t}_i \rangle = \mathbf{n}_i \cdot \boldsymbol{\sigma}^\infty$) is readily recovered by taking all transmission factors $\Lambda_{ik} = 0$ (no interactions) so that $\boldsymbol{\Omega}_{ik} = \delta_{ik}\mathbf{I}$. We remark that taking Λ's in the approximation of remotely located cracks (Section 6) yields a *rigorous* first-order correction to $\mathbf{C}^{\text{eff}}$ due to crack interactions. Note that this first-order correction will already depend not only on the density of cracks and their orientations but on their *mutual positions* within the elementary volume as well.

Since the presented approach to many crack problems is accurate at quite close distances between cracks, the results for the effective elastic properties can be expected to be accurate up to high crack densities. Unlike some of the existing models for the effective properties, these results will be sensitive to mutual locations of cracks. Formulas (31) and (33) assume that the information on the crack array geometry is known in deterministic terms; statistical information on the crack array can be incorporated into the model through the statistical treatment of the transmission factors.

10. INTERACTION OF A CRACK WITH A MICROCRACK ARRAY

This problem models interaction of a crack with a damage field developing in a process zone near the crack tip in many brittle materials[16, 17]. Such an interaction can significantly alter the stress concentration at the main crack tip. Depending on geometry of the microcrack array, both stress amplification and stress shielding (increase or decrease of the effective SIF) can occur. (The problem has been approached by the polynomial approximations technique in Refs [4–6] where two simple examples were also considered.)

The configuration consists of a semi-infinite crack and a microcrack array. The stress field can be represented as a superposition

$$\boldsymbol{\sigma}(\mathbf{x}) = K_{\text{I}}\boldsymbol{\sigma}_{\text{I}}(\mathbf{x}) + K_{\text{II}}\boldsymbol{\sigma}_{\text{II}}(\mathbf{x}) + \sum_{i=1}^{N} \boldsymbol{\sigma}_i(\mathbf{x}) \tag{34}$$

(N is the number of microcracks) where $\boldsymbol{\sigma}_{\text{I}} = \mathbf{f}_{\text{I}}(\theta)/\sqrt{(2\pi r)}$ and $\boldsymbol{\sigma}_{\text{II}} = \mathbf{f}_{\text{II}}(\theta)/\sqrt{(2\pi r)}$ denote modes I and II asymptotic crack tip fields and $\boldsymbol{\sigma}_i$ is the ith microcrack-generated stress. Applying our method we represent the traction $\mathbf{t}_i(\xi)$ on the ith microcrack as a sum of tractions induced by the other microcracks loaded by the average tractions on them plus

the traction induced by the main crack tip (analogously to eqns (13a), with the main crack tip field playing the role of σ^∞)

$$\mathbf{t}_i(\xi) = \mathbf{n}_i \cdot \{K_\mathrm{I}\boldsymbol{\sigma}_\mathrm{I} + K_\mathrm{II}\boldsymbol{\sigma}_\mathrm{II} + \sum_k (\langle p_k \rangle \boldsymbol{\sigma}_k^n + \langle \tau_k \rangle \boldsymbol{\sigma}_k^\tau)\}. \tag{35}$$

taking the average of eqn (35) over 1_i yields

$$\langle \mathbf{t}_i \rangle = \boldsymbol{\phi}_i K_\mathrm{I} + \boldsymbol{\psi}_i K_\mathrm{II} + \sum \boldsymbol{\Lambda}_{ik} \cdot \langle \mathbf{t}_k \rangle \tag{36}$$

where the transmission $\boldsymbol{\Lambda}$-factors interrelate average tractions on different microcracks and vectors $\boldsymbol{\phi}_i = \mathbf{n}_i \cdot \langle \boldsymbol{\sigma}_\mathrm{I} \rangle_i$, $\boldsymbol{\psi}_i = \mathbf{n}_i \cdot \langle \boldsymbol{\sigma}_\mathrm{II} \rangle_i$ characterize the impact of modes I and II on the main crack on the average traction on the ith microcrack, respectively.

N vectorial linear algebraic equations (36) contain N vectorial unknowns $\langle \mathbf{t}_k \rangle$ and two unknown scalars K_I, K_II. Two additional scalar equations express the impact of microcracks on the main crack

$$\left.\begin{aligned} K_\mathrm{I} &= K_\mathrm{I}^0 + \sqrt{(2/\pi)} \int_0^\infty \xi^{-1/2} \sum_i \sigma_{(i)yy}(\xi)\, \mathrm{d}\xi \\ K_\mathrm{II} &= K_\mathrm{II}^0 + \sqrt{(2/\pi)} \int_0^\infty \xi^{-1/2} \sum_i \sigma_{(i)xy}(\xi)\, \mathrm{d}\xi \end{aligned}\right\} \tag{37}$$

where K_I^0, K_II^0 denote SIFs on the main crack in the absense of microcracks. Solving eqns (36) and (37) yields SIFs at the main crack tip (and the average tractions on microcracks). If, in addition, SIFs at the *micro*crack tips are of interest, they are obtained as induced by tractions $\mathbf{t}_i$ given by eqn (35).

Simplicity of the method allows one to analyze interaction of the main crack with arbitrary microcrack patterns. Two test configurations—one collinear microcrack and a periodic row of collinear microcracks—for which the exact solutions exist[20] show that the results remain quite accurate when the spacings between cracks are much smaller than the microcrack length. For more detailed analysis of various configurations, see Refs [18, 19]. Some important features of the crack–microcrack array interactions can be summarized as follows. Under mode I loading conditions, the effect of shielding ("toughening by microcracking") is generally dominant, as compared to the one of amplification. The opposite appears to be true in mode II loading. The effect of microcracks located "behind" the main crack tip ("passive" part of the fracture zone) is very small.

Three-dimensional crack–microcrack interactions can be analyzed along the same lines, by taking $\boldsymbol{\sigma}_i$ as the "standard" stress fields generated by uniformly loaded microcracks (penny-shaped or elliptical) and using the 3-D analogue of formulas (37) for the SIFs along the edge of the main crack (penny-shaped or elliptical).

11. COMPARISON WITH THE POLYNOMIAL APPROXIMATION TECHNIQUES. DISCUSSION

The advantages of the presented method are that it is simple and applies to both 2-D and 3-D configurations with equal ease. It is interesting to compare the results produced by our method with the ones obtained by the polynomial approximations techniques (see Introduction).

Taylor's polynomials centered at the crack centers represent the simplest choice of approximating polynomials. They were applied to the configuration "crack–microcrack array" in Refs [4–6] and to the general 2-D crack array by Horii and Nemat-Nasser[7, 8]. The latter authors considered the same test problems—two collinear cracks and a periodic row of collinear cracks—as in Sections 2 and 3. Their results show that the degree of approximating polynomials increases rapidly as the spacings between cracks become

smaller. The closest distance considered in Refs [7,8] is 1/4 of the crack length; at this distance the polynomials' degrees are 28 and 17 for the problems of two collinear cracks and a periodic row of cracks, respectively (for the latter problem, the results obtained by using linear and quadratic polynomials are also given; they generate errors of 15 and 7%). At this distance, our method yields practically indistinguishable errors (about 0.3%). At the distances one order of magnitude smaller than the crack length, the polynomial's degree in the method of polynomial approximations can be expected to be several times higher; for an arbitrary array of N cracks under mixed loading conditions, the total number of polynomials' coefficients to be determined will have to be multiplied by $2N$.

Gross[3] showed that the Chebyshev's polynomials represent the best choice of approximating polynomials (in the sense that the increase of the polynomials' degree by one increases the rate of attenuation of error of the crack-generated stress with distance by r^{-1}). The technique of Chebyshev's polynomials was applied to the problem of two collinear cracks by Lietzau[21] who found that, similarly to the Taylor's polynomials technique, convergence becomes increasingly difficult as the spacings between cracks become smaller. The closest distance considered in Ref. [21] was 1/10 of the crack length; at this distance, the Chebyshev's polynomials of the sixth degree yield a 10.7% error in SIFs; for comparison, our method yields a 1.5% error (Table 1).

It seems that the key difficulty in polynomial approximations of tractions (induced on a given crack line by the other cracks) is that these tractions are *singular* (at the other cracks' tips). At small distances between cracks such approximations become increasingly difficult. The above proposed method, on the other hand, takes these tractions as "standard" fields (generated by the other cracks) and thus retains the singularities.

Note that the technique of polynomial approximations, as presented in Refs [3,7–9] is based on complex variables representations and is not, therefore, easily extendable to the 3-D configurations. Such an extension is possible by coupling polynomial approximations with the integral representations of the double layer potential type ("representation of cracks by dislocations"), as suggested in Refs [4–6]. The main drawback of the polynomial technique—a large number of polynomial coefficients (rapidly increasing as spacings between cracks become smaller)—will, however, become much more severe in the 3-D problems where polynomials of *two* variables will have to be used for approximation of tractions on each of the cracks.

The advantages of the proposed method, as compared to the polynomial approximations technique, may under certain conditions be less pronounced in the problem of "crack–microcrack array" interactions. If microcracks are much smaller than the main crack and are not too close to it, then the main crack-generated stresses can be taken as approximately constant along each of the microcracks. Furthermore, if the interactions *between* microcracks are weak as compared to their interactions with the main crack tip, then the total tractions on each of the microcracks are approximately constant and the problem formulated by eqns (36) and (37) is reduced to interrelating these constants and K_{I}, K_{II}. The mentioned constants should be taken as traction *averages*; substitution of the latter by the traction values at the microcrack *centers* (may result in insignificant errors) constitutes the zeroth order Taylor's polynomials approximation (called "piecewise constant" approximation in earlier work[4–6] where higher order Taylor's approximations are also considered).

The key idea of the proposed method—to neglect the impact on a given crack of the traction nonuniformities on the other cracks—is somewhat similar to the Saint–Venant's principle of elasticity and may be interpreted as the Saint–Venant-type principle for solids with cracks. Moreover, since the SIFs are given by *integrals* of tractions (eqn (14) or its 3-D analogue), the effect of the mentioned nonuniformities is neglected not in the pointwise sense (as in Saint–Venant's principle) but in a "milder", integral sense. This may explain why our principle works well for closely spaced cracks.

The method allows further refinements. For example, in addition to the average tractions, linear components of the traction nonuniformities (having zero average) can be taken into account. Then, in addition to the transmission factors interrelating the traction

averages on the cracks ("average → average" interactions), factors of the type "average → linear", "linear → linear", "linear → average" are to be introduced; they will be determined from a system of linear algebraic equations. The next term—the quadratic component of the traction nonuniformities—can also be taken into account; it may be relevant for an array of cracks with symmetrically distributed tractions on them when the linear component vanishes (periodic arrays, for instance). Another way to improve accuracy is to construct the CODs as "quadratically distorted" ellipses matching the SIFs and the average tractions, eqns (22) and (23), and, substituting them into eqn (21), recalculate the tractions induced on a given crack by the other cracks. The formulas given in the appendix provide the ingredients necessary for the mentioned refinements. The accuracy will be improved even further, but at the expense of simplicity. The test problems considered above seem to indicate that the simplest version of the method is, typically, adequate.

Note that our model is linear elastic and, therefore, does not describe the nonlinearities related to a (possibly) different behavior of a crack in tension and compression in the direction normal to the crack faces. The existence of such nonlinearity depends on the level of compressive stresses and the initial aspect ratio of the crack: at low compressive stresses insufficient to close the crack (some stress waves problems, etc.) the linear elastic model is adequate; at higher compressive stresses, gradual closing of a crack results in a nonlinearity. For very thin cracks, this nonlinearity can be approximated by a piecewise-linear behavior. The latter can be incorporated into our method by eliminating the mode I component σ^n of the crack-generated stresses for the cracks with negative $\langle p \rangle$ (leaving the mode II component σ^τ unchanged under conditions of no friction or setting $\sigma^\tau = 0$ under conditions of high friction inhibiting sliding of the crack faces) and reconsideration of system (13b).

Note, also, that the method appears to be suited for incorporation of the statistical information on the crack array (through statistical treatment of the transmission factors).

Acknowledgements—Support of the Army Research Office (Grant DAAG29-84-K-0184) and of the Air Force Office of Scientific Research (Grant AFOSR-84-0321) is gratefully acknowledged.

REFERENCES

1. M. Kachanov, A simple technique of stress analysis in elastic solids with many cracks. *Int. J. Fracture* **28**, R11–R19 (1985).
2. A. P. Datsyshin and M. P. Savruk, A system of arbitrarily oriented cracks in elastic solids. *J. Appl. Math. Mech.* (*PMM*, translation of the Soviet journal *Prikl. Mat. Mekh.*) **37**(2), 326–332 (1973).
3. D. Gross, Spannungsintensitätsfaktoren von Ribsystemen (Stress intensity factors of systems of cracks). *Ing.-Arch.* **51**, 301–310 (1982) (in German).
4. A. Chudnovsky and M. Kachanov, Interaction of a crack with a field of microcracks, *Int. J. Engng Sci.* **21**(8), 1009–1018 (1983).
5. A. Chudnovsky, A. Dolgopolsky and M. Kachanov, Elastic interaction of a crack with microcracks, in *Advances in Fracture Research. Proc. Sixth Conf. on Fracture, New Delhi, India* (Edited by S. R. Valluri *et al.*), Vol. 2, pp. 825–833 (1984).
6. A. Chudnovsky, A Dolgopolsky and M. Kachanov, Elastic interaction of a crack with a microcrack array—Parts I and II. *Int. J. Solids Structures* **23**, 1–10, 11–21 (1987).
7. H. Horii and S. Nemat-Nasser, Estimate of stress intensity factors for interacting cracks, in *Advances in Aerospace Structures, Materials and Dynamics* (Edited by U. Yuceoglu *et al.*), pp. 111–117. ASME (1983).
8. H. Horii and S. Nemat-Nasser, Elastic fields of interacting inhomogeneities. *Int. J. Solids Structures* **21**, 731–745 (1985).
9. Y. Z. Chen, General case of multiple crack problems in an infinite plate. *Engng Fracture Mech.* **20**, 591–597 (1984).
10. W. D. Collins, Some axially symmetric stress distributions in elastic solids containing penny-shaped cracks. *Proc. R. Soc., Ser. A* **266**(1324), 359–386 (1962).
11. H. Tada, P. C. Paris and G. R. Irwin, *The Stress Analysis of Cracks Handbook*. Del Research Corp., Hellertown, Pennsylvania (1973).
12. I. N. Sneddon and M. Lowengrub, *Crack Problems in the Classical Theory of Elasticity*. Wiley, New York (1969).
13. G. C. Sih, *Handbook of Stress Intensity Factors*. Lehigh University, Bethlehem, Pennsylvania (1973).
14. R. Hill, A self-consistent mechanics of composite materials. *J. Mech. Phys. Solids* **13**, 213–222 (1965).
15. Z. Hashin, Analysis of composite materials—a survey. *J. Appl. Mech.* **50**, 487–505 (1983).
16. C. Wu, S. Freiman, R. Rice and J. Mecholsky, Microstructural aspects of crack propagation in ceramics. *J. Mater. Sci.* **13**, 2659–2670 (1978).
17. A. Carpinteri and A. Ingraffea (Editors), *Fracture Mechanics of Concrete*. Martinus Nijhoff, The Hague (1984).

18. M. Kachanov, Elastic interaction of a crack with certain microcrack arrays. *Engng Fracture Mech.* (1987), in press.
19. M. Kachanov, On crack–microcrack interactions. *Int. J. Fracture* **30**, R65–R72 (1986).
20. A. Rubinstein, Macrocrack interaction with semi-infinite microcrack array. *Int. J. Fracture* **27**, 113–119 (1985).
21. H. P. Lietzau, M.S. Thesis, Darmstadt Polytechnic Institute (1986).

APPENDIX

A quadratic loading

$$p(x) = p_0\left(1 + \alpha\frac{x}{l} + \beta\frac{x^2}{l^2}\right) \tag{A1}$$

on a crack $(-l, l)$ results in the following SIFs

$$K_I(\pm l) = \frac{1}{\sqrt{(\pi l)}}\int_{-l}^{l} p(x)\sqrt{\left(\frac{l \pm x}{l \mp x}\right)}\,dx = p_0\sqrt{(\pi l)}\left(1 \pm \frac{\alpha}{2} + \frac{\beta}{2}\right)$$

and has an average

$$p(x) = \frac{1}{2l}\int_{-l}^{l} p(x)\,dx = p_0\left(1 + \frac{\beta}{3}\right).$$

Equations (23) are based on these formulas and on a relation between the loading (A1), and COD derived below.

A simple way to derive the COD corresponding to the loading (A1), is by using Castigliano's theorem (see, e.g. Ref. [11]). To calculate the opening $b(x)$ at a certain point x we apply a couple of virtual forces Q at this point. If $K_{Ip}(\pm l)$ and $K_{IQ}(\pm l)$ are the SIFs corresponding to the actual loading $p(x)$ and to Q, then, by considering the crack as having grown symmetrically from $x = 0$, calculating the energy release contributions from both crack tips and letting the virtual forces Q approach zero we find

$$b(x) = \frac{2}{E'}\int_{x}^{l}\left[K_{Ip}(l')\frac{\partial K_{IQ}(l')}{\partial Q} + K_{Ip}(-l')\frac{\partial K_{IQ}(-l')}{\partial Q}\right]dl'.$$

Substitution of

$$K_{Ip}(\pm l') = p_0\sqrt{(\pi l')}\left(1 \pm \frac{\alpha_n}{2} + \frac{\beta_n}{2}\right)$$

and

$$K_{IQ}(\pm l') = \frac{Q}{\sqrt{(\pi l')}}\sqrt{\left(\frac{l' \pm x}{l' \mp x}\right)}$$

and integration establishes a relation between the coefficients of the quadratic loading (A1), and the coefficients of a "quadratic distortion" of an elliptical COD

$$b(x) = \frac{4p_0 l}{E'}\left(1 + \frac{\beta_n}{6} + \frac{\alpha_n}{2}\frac{x}{l} + \frac{\beta_n}{3}\frac{x^2}{l^2}\right)\sqrt{\left(1 - \frac{x^2}{l^2}\right)}. \tag{A2}$$

(A similar relation holds for mode II loading, with p_0 changed to τ_0 and α_n, β_n changed to α_τ, β_τ.) The stress field generated by the crack can now be found by using $b(x)$ in eqn (21). Transformation of the displacement field into stresses $\sigma_{ij}(u) = \lambda u_{k,k}\delta_{ij} + \mu(u_{i,j} + u_{j,k})$ will require differentiation of the second Green's tensor

$$\mathbf{\Phi}(\boldsymbol{\xi}, \mathbf{x}) = \frac{1 + \nu}{4\pi R^2}\left[(1 - 2\nu)(\mathbf{nR} - \mathbf{Rn} - \mathbf{n}\cdot\mathbf{RI}) - 2\mathbf{n}\cdot\mathbf{R}\frac{\mathbf{RR}}{R^2}\right] \quad \text{(plane stress†)}$$

where $\mathbf{R} = \boldsymbol{\xi} - \mathbf{x}$, $\mathbf{I} = \mathbf{e}_1\mathbf{e}_1 + \mathbf{e}_2\mathbf{e}_2$ is a 2-D unit tensor and $\mathbf{n}$ is, in our case, a unit normal to the crack. The σ_{yy} stress component, for example, is

† For plane strain, the factor $1 + \nu$ is to be changed to $1/(1 - \nu)$.

$$\sigma_{yy} = \int_{-l}^{l} b(\xi)[(\lambda + 2\mu)\Phi_{22,2} + \lambda\Phi_{21,1}]\,d\xi.$$

Evaluation of the integrals in eqn (21) by the residue technique yields the expressions for stresses. They can be represented as a sum of the stress fields corresponding to the constant, $p_0(1 + \beta/6)$, linear, $p_0(\alpha/2 \times x/l)$ and quadratic, $p_0(\beta/3 \times x^2/l^2)$ terms of the "distorsion polynomial" (A2). The stresses due to the constant terms (can also be found in Ref. [12]) are of particular importance: they are the "standard" stress fields σ^n and σ^τ used throughout the presentation. These fields as well as the fields due to linear, x/l, and quadratic, x^2/l^2, terms are given below for each of the modes I and II.

Mode I loading

(1) Stress field generated by a uniform load of unit intensity ("standard" stress field σ^n)

$$\sigma_{xx} = I_2 - 8y^2 I_4 + 8y^4 I_6$$
$$\sigma_{xy} = 2(-yI_3 + xyI_4 + 4y^3 I_5 - 4xy^3 I_6)$$
$$\sigma_{yy} = I_2 + 6y^2 I_4 - 8y^4 I_6.$$

(2) Stress field generated by a linear (x/l) term

$$\sigma_{xx} = \frac{1}{l}(I_1 - 8y^2 I_3 + 8y^4 I_5)$$
$$\sigma_{xy} = \frac{2}{l}[-yI_2 - xyI_3 + y(x^2 + 5y^2)I_4 + 4xy^3 I_5 - 4y^3(x^2 + y^2)I_6]$$
$$\sigma_{yy} = \frac{1}{l}(I_1 + 6y^2 I_3 - 8y^4 I_5).$$

(3) Stress field generated by a quadratic (x^2/l^2) term

$$\sigma_{xx} = \frac{1}{l^2}\left[\frac{l^2}{2} + 2xI_1 - (x^2 + 9y^2)I_2 - 16xy^2 I_3 + 8y^2(x^2 + 2y^2)I_4 + 8xy^4 I_5 - 8y^4(x^2 + y^2)I_6\right]$$
$$\sigma_{xy} = \frac{2}{l^2}\left[-yI_1 - xyI_2 + y(-x^2 + 5y^2)I_3 + xy(x^2 + 5y^2)I_4 + 4y^3(x^2 - y^2)I_5 - 4xy^3(x^2 + y^2)I_6\right]$$
$$\sigma_{yy} = \frac{1}{l^2}\left[\frac{l^2}{2} + 2xI_1 + (-x^2 + 3y^2)I_2 + 8xy^2 I_3 - 4y^2(x^2 + 3y^2)I_4 - 8xy^4 I_5 + 8y^4(x^2 + y^2)I_6\right]$$

Mode II loading

(1) Stress field generated by a uniform load of unit intensity ("standard" stress field σ^τ)

$$\sigma_{xx} = 2(3yI_3 - 3xyI_4 - 4y^3 I_5 + 4xy^3 I_6)$$
$$\sigma_{xy} = I_2 - 8y^2 I_4 + 8y^4 I_6$$
$$\sigma_{yy} = 2(-yI_3 + xyI_4 + 4y^3 I_5 - 4xy^3 I_6).$$

(2) Stress field generated by a linear (x/l) term

$$\sigma_{xx} = \frac{2}{l}[3y^2 I_2 + 3xyI_3 - y(3x^2 + 7y^2)I_4 - 4xy^3 I_5 + 4y^3(x^2 + y^2)I_6]$$
$$\sigma_{xy} = \frac{1}{l}(I_1 - 8y^2 I_3 + 8y^4 I_5)$$
$$\sigma_{yy} = \frac{2}{l}[-yI_2 - xyI_3 + y(x^2 + 5y^2)I_4 + 4xy^3 I_5 - 4y^3(x^2 + y^2)I_6].$$

(3) Stress field generated by a quadratic (x^2/l^2) term

$$\sigma_{xx} = \frac{2}{l^2}[3yI_1 + 3xyI_2 + y(3x^2 - 7y^2)I_3 - xy(3x^2 + 7y^2)I_4 - 4y^3(x^2 - y^2)I_5 + 4xy^3(x^2 + y^2)I_6]$$
$$\sigma_{xy} = \frac{1}{l^2}\left[\frac{l^2}{2} + 2xI_1 - (x^2 + 9y^2)I_2 - 16xy^2 I_3 + 8y^2(x^2 + 2y^2)I_4 + 16xy^4 I_5 - 8y^4(x^2 + y^2)I_6\right]$$
$$\sigma_{yy} = \frac{2}{l^2}[-yI_1 - xyI_2 - y(x^2 - 5y^2)I_3 + xy(x^2 + 5y^2)I_4 + 4y^3(x^2 - y^2)I_5 - 4xy^3(x^2 + y^2)I_6]$$

The following notations are used in the above formulas

$$I_1 = 4l^3 \frac{\sqrt{\gamma} - \sqrt{\alpha}}{\sqrt{\delta}(\sqrt{\alpha} + \sqrt{\gamma} + \sqrt{\delta})^2}$$

$$I_2 = 4l^2 \frac{1}{\sqrt{\delta}(\sqrt{\alpha} + \sqrt{\gamma} + \sqrt{\delta})}$$

$$I_3 = 2l^3 \frac{\sqrt{\gamma} - \sqrt{\alpha}}{\sqrt{(\alpha\gamma)}\delta^{3/2}}$$

$$I_4 = 2l^2 \frac{\sqrt{\alpha} + \sqrt{\gamma}}{\sqrt{(\alpha\gamma)}\delta^{3/2}}$$

$$I_5 = \frac{l^3}{2} \frac{3\sqrt{(\alpha\gamma)}(\sqrt{\alpha} + \sqrt{\gamma})^2(\sqrt{\gamma} - \sqrt{\alpha}) + \delta(\gamma^{3/2} - \alpha^{3/2})}{(\alpha\gamma)^{3/2}\delta^{5/2}}$$

$$I_6 = \frac{l^2}{2} \frac{(\alpha^{3/2} + \gamma^{3/2})\delta + 3\sqrt{(\alpha\gamma)}(\sqrt{\alpha} + \sqrt{\gamma})^3}{(\alpha\gamma)^{3/2}\delta^{5/2}}$$

where

$$\alpha = (x - l)^2 + y^2$$
$$\beta = 2(x^2 + y^2 - l^2)$$
$$\gamma = (x + l)^2 + y^2$$
$$\delta = \beta + 2\sqrt{(\alpha\gamma)}.$$

In the 3-D case, the stress field generated by a penny-shaped crack of radius a loaded by a uniform normal traction p is found from the same representation, eqn (21), as in the 2-D case, with

$$\Phi(\xi, \mathbf{x}) = \frac{1}{8\pi(1-\nu)} \frac{1}{R^3} \left[(1 - 2\nu)(\mathbf{nR} - \mathbf{Rn} - \mathbf{n} \cdot \mathbf{RI}) - 3\mathbf{n} \cdot \mathbf{R} \frac{\mathbf{RR}}{R^2} \right]$$

(where $\mathbf{I} = \mathbf{e}_1\mathbf{e}_1 + \mathbf{e}_2\mathbf{e}_2 + \mathbf{e}_3\mathbf{e}_3$, otherwise notations are the same as in the 2-D case). Making use of the ellipsoidal COD due to loading p

$$b(x_\xi, y_\xi) = \frac{8(1-\nu^2)a}{\pi E} p \sqrt{\left(1 - \frac{x_\xi^2}{a^2} - \frac{y_\xi^2}{a^2}\right)}$$

performing differentiation of Φ (required by transformation of displacements $\mathbf{u}$ into stresses) and integration yield the stress field. In particular, the stress σ_{zz} normal to the crack is given by

$$\sigma_{zz}(x, y, z) = \frac{8(1-\nu^2)a}{\pi E} p \int_S \sqrt{\left(1 - \frac{x_\xi^2}{a^2} - \frac{y_\xi^2}{a^2}\right)} [(\lambda + 2\mu)\Phi_{33,3} + \lambda(\Phi_{31,1} + \Phi_{32,2})] \, dS_\xi.$$

Evaluation of the integral along the Z-axis and in-plane of the crack yield expressions (16) and (19).